Molecular Dynamics Simulation of Structural Transformation in Silicon Carbide under Pressure

Fuyuki Shimojo,[1,2] Ingvar Ebbsjö,[3] Rajiv K. Kalia,[1] Aiichiro Nakano,[1] Jose P. Rino,[1,4] and Priya Vashishta[1]

[1]*Concurrent Computing Laboratory for Materials Simulations, Department of Physics and Astronomy and Department of Computer Science, Louisiana State University, Baton Rouge, Louisiana 70803*

[2]*Faculty of Integrated Arts and Sciences, Hiroshima University, Higashi-Hiroshima 739-8521, Japan*

[3]*Studsvik Neutron Research Laboratory, University of Uppsala, Nyköping, Sweden*

[4]*Department of Physics, Universidade Federal de São Carlos, São Carlos, São Paulo, Brazil*

(Received 12 November 1999)

Pressure-induced structural transformation in cubic silicon carbide is studied with the isothermal-isobaric molecular-dynamics method using a new interatomic potential scheme. The reversible transformation between the fourfold coordinated zinc-blende structure and the sixfold coordinated rocksalt structure is successfully reproduced by the interatomic potentials. The calculated volume change at the transition and hysteresis are in good agreement with experimental data. The atomistic mechanisms of the structural transformation involve a cubic-to-monoclinic unit-cell transformation and a relative shift of Si and C sublattices in the {100} direction.

PACS numbers: 61.50.Ks, 64.70.Kb, 62.20.Dc

The importance of silicon carbide (SiC) has been emphasized for a wide range of technological applications, such as optoelectronic devices and engineering materials, because it has highly useful properties, i.e., excellent chemical stability, good electronic properties, high stiffness, and high hardness. At ambient pressure, there exist various polytypes in SiC originating from differences in the stacking sequence of the silicon-carbon pair layer [1,2]. In all these polytypes, the chemical bonds characterized by covalent sp^3 bonding are identical and the tetrahedrally coordinated properties are almost the same [3]. Among the polytypes, the zinc-blende structure is most common.

It is important to study the phase stability of materials under high pressures for microscopic understanding as well as technological applications [4]. For the last few decades, there have been a number of experimental [5–7] and theoretical [8–10] studies on the high-pressure properties of SiC. Yoshida *et al.* [6] have found from x-ray diffraction measurements that SiC transforms from the fourfold coordinated zinc-blende structure to a sixfold coordinated rocksalt structure at a pressure above 100 GPa, with a 20.3% volume reduction. Their measurements have observed a large hysteresis associated with this phase transition; when the pressure is decreased, a backward transformation from the rocksalt structure to the zinc-blende structure takes place at a pressure below 35 GPa. Shock compression experiments [7] also suggest that the high-pressure phase of SiC above 100 GPa has rocksalt structure. Theoretical studies [8–10] based on *ab initio* pseudopotential calculations predict the transition pressure to be around 60 GPa, which is in reasonable accord with experiments. No simulation studies of structural transformation in SiC are reported so far and the mechanism of transformation at the atomistic level is not well understood, although the structural properties of SiC in the zinc-blende structure have been investigated extensively not only by *ab initio* methods but also by empirical models [11].

In this paper, we report the results of isothermal-isobaric molecular-dynamics (MD) simulations [12–16] for the pressure-induced structural transformation in SiC. The equations of motion are integrated by a reversible symplectic algorithm [17] with a time step of 0.96 fs. The system consists of 1728 atoms, and we use the periodic boundary conditions.

The total interatomic potential involves both two-body and three-body terms [18,19],

$$V = \sum_{i<j} V_{ij}^{(2)}(r_{ij}) + \sum_{i,j<k} V_{jik}^{(3)}(\mathbf{r}_{ij}, \mathbf{r}_{ik}) . \qquad (1)$$

The two-body terms include effects of steric repulsion, charge transfer between atoms, charge-dipole interactions, and van der Waals interactions:

$$V_{ij}^{(2)}(r_{ij}) = \frac{H_{ij}}{r_{ij}^{n_{ij}}} + \frac{Z_i Z_j}{r_{ij}} e^{-r_{ij}/a} - \frac{D_{ij}}{r_{ij}^4} e^{-r_{ij}/b} - \frac{W_{ij}}{r_{ij}^6} . \qquad (2)$$

The first term due to steric repulsion contains two parameters (H_{ij}) and (n_{ij}); the second term represents Coulomb interaction due to charge transfer and contains the effective atomic charges (Z_i) as parameters; the third term takes into account the charge-dipole interaction due to large polarizability of negative ions; and the last term, corresponding to the induced dipole-dipole interaction, contains the parameter (W_{ij}). Covalent effects are taken into account through three-body bond-bending and bond-stretching terms. The three-body term $V_{jik}^{(3)}$ includes the Si-C-Si and C-Si-C bond angles. It has the form

$$V_{jik}^{(3)}(\mathbf{r}_{ij}, \mathbf{r}_{ik}) = B_{jik} \exp\left(\frac{\gamma}{r_{ij} - r_0} + \frac{\gamma}{r_{ik} - r_0}\right) \times \frac{(\cos\theta_{jik} - \cos\overline{\theta}_{jik})^2}{1 + C(\cos\theta_{jik} - \cos\overline{\theta}_{jik})^2} \times \Theta(r_0 - r_{ij})\Theta(r_0 - r_{ik}) , \qquad (3)$$

where B_{jik} is the strength of the interaction,

 0031-9007/00/84(15)/3338(4)$15.00

TABLE I. Molecular-dynamics results and experimental values for lattice constant, elastic constants c_{11}, c_{12}, and c_{44}, bulk modulus, and melting temperature.

	MD	Experiments
Lattice constant (Å)	4.36	4.36[a]
Elastic constants (GPa)		
c_{11}	390	390[a]
c_{12}	144	142[a]
c_{44}	179	150[b]–256[a]
Bulk modulus (GPa)	225	225[a]
Melting/decomposition temperature (°C)	3000	2830[a]

[a]Reference [14]; [b]Ref. [15].

$\Theta(r_0 - r_{ij})\Theta(r_0 - r_{ik})$ are step functions, and $\overline{\theta}_{jik}$ is a constant. Here θ_{jik} is the angle formed by $\mathbf{r}_{ij}$ and $\mathbf{r}_{ik}$. For structural transformations the constant C in the three-body term plays an important role. The cutoff lengths for the two- and three-body terms are 7.5 and 4.0 Å, respectively. Physical properties including lattice constant, elastic constants C_{11}, C_{12}, an C_{44}, and bulk modulus are in excellent agreement with the experimental data [20,21]. The melting or decomposition temperature and the phonon density of states obtained by MD simulations are also in good accord with experiments. These theoretical values are compared with experimental data in Table I. Figure 1 shows a comparison between MD and experimental results for the volume-pressure relationship in SiC in the zinc-blende structure. The MD results agree well with the experiments [5] in a wide range of pressure. From a common-tangent construction using the calculated energy-volume relationship for crystalline SiC in Fig. 2, the transition pressure is estimated to be about 100 GPa, which is in excellent agreement with experimental values [6].

In our MD simulations for structural transformation, the temperature was set to room temperature (300 K). The pressure was increased from 0 to 140 GPa at a rate of 10 GPa per 19.2 ps. Figure 3 shows the time evolution of the MD cell vectors and angles between them at 140 GPa. Up to 130 GPa, the form of MD cell is cubic, and the system remains the zinc-blende structure. When the pressure is increased to 140 GPa, a structural transformation occurs, which is characterized by a change in MD cell lengths and angles, in Fig. 3. One MD cell vector shortens, while the others lengthen. As for the angles between MD cell vectors, one angle is decreased to about 70°, while the others keep right angles. These observations indicate that the MD cell transforms from cubic to monoclinic. The volume of the zinc-blende structure at 130 GPa just before the transition is $0.78V_0$ (V_0 is the volume at the ambient pressure), and the volume reduction accompanying the transition is 21%. These MD results agree well with the experimental values, $0.757V_0$ and 20.3%, respectively [6].

Figure 4 shows the Si-C pair distribution functions and the coordination number around Si and C before and after the transition. The nearest-neighbor coordination numbers are 4 and 6 before and after the transformation, respectively. This clearly demonstrates the structural transformation from a fourfold coordinated structure to a sixfold coordinated structure under pressure.

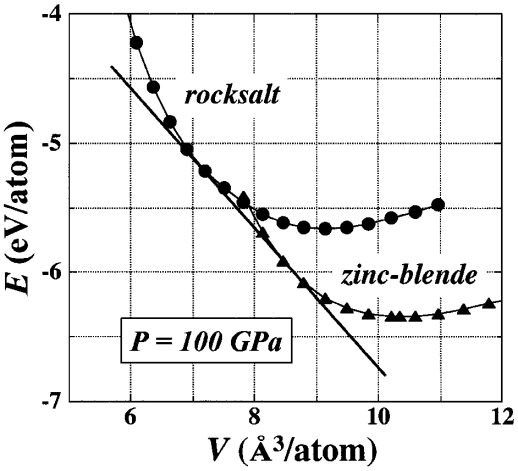

FIG. 2. Energy-volume relation for the crystalline SiC calculated by the present interatomic potentials. The triangles correspond to the zinc-blende structure, and the circles correspond to the rocksalt structure. From these curves, the transition pressure is estimated to be about 100 GPa being in agreement with the experiments [6].

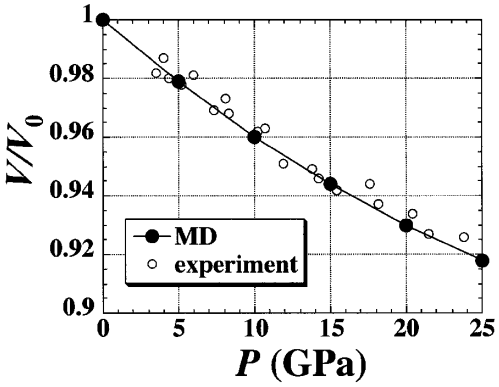

FIG. 1. Volume-pressure relation for zinc-blende structure. The solid circles are the results of the MD simulation, and the open circles are the experimental results [5].

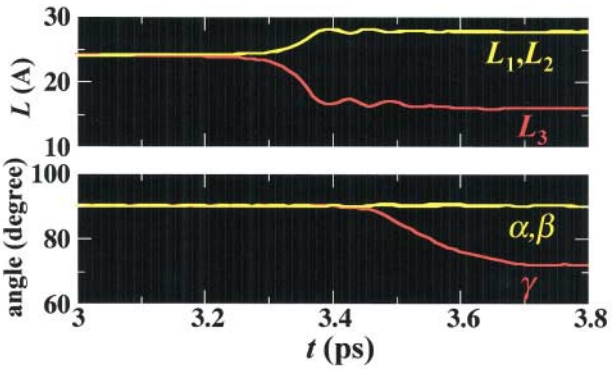

FIG. 3 (color). Time change of the MD cell vectors (upper portion) and angles between them (lower portion) at 140 GPa.

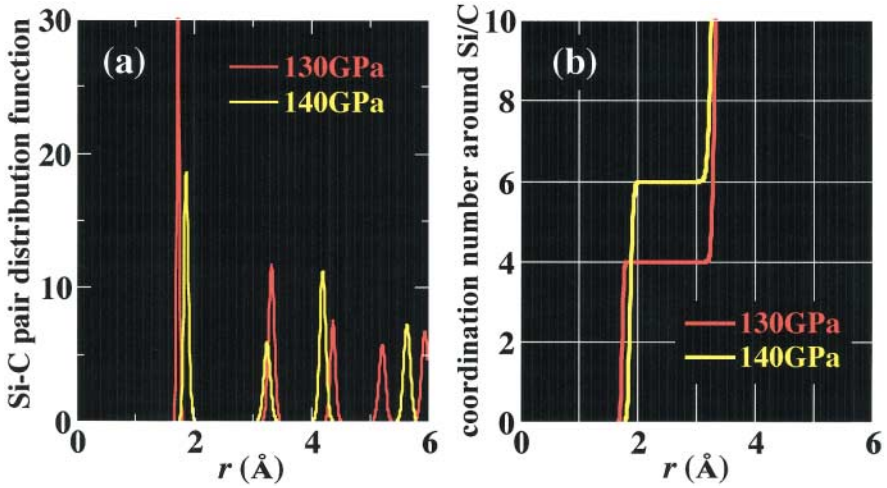

FIG. 4 (color). (a) The Si-C pair distribution functions and (b) the coordination number around Si and C. In both figures, the red line shows the correlations before the transformation (130 GPa), and the yellow line shows the correlations after the transformation (140 Pa).

In order to determine the exact structures before and after the transition, we calculated the average positions of atoms in the MD cell as shown in Fig. 5. Before the transition, the MD cell is cubic, and the unit cell vectors **a**, **b**, and **c** of the zinc-blende structure are parallel to the MD cell vectors $\mathbf{L}_1$, $\mathbf{L}_2$, and $\mathbf{L}_3$. Therefore, we can easily determine the unit cell vectors using the following relations: $\mathbf{a} = \mathbf{L}_1/6$, $\mathbf{b} = \mathbf{L}_2/6$, $\mathbf{c} = \mathbf{L}_3/6$. After the transition, the MD cell is deformed to monoclinic as shown in Fig. 5. In this case, we can calculate the size and shape of the unit cell by using the following relations: $\mathbf{a} = (\mathbf{L}_1 + \mathbf{L}_2)/12$, $\mathbf{b} = (-\mathbf{L}_1 + \mathbf{L}_2 + 2\mathbf{L}_3)/12$, $\mathbf{c} = (\mathbf{L}_1 - \mathbf{L}_2 + 2\mathbf{L}_3)/12$. Using the time averaged values of $\mathbf{L}_1 = (27.613, 0.000, 0.000)$, $\mathbf{L}_2 = (9.204, 26.034, 0.000)$, and $\mathbf{L}_3 = (0.000, 0.000, 15.941)$ in angstroms, we confirm that the unit cell vectors are perpendicular to each other, and the rocksalt structure is obtained.

A previously proposed atomistic mechanism for the structural transformation from the zinc-blende to rocksalt structures is as follows [10]. In both the zinc-blende and rocksalt structures, Si and C sublattices form the fcc structure. If each sublattice in the zinc-blende structure shifts to the {111} direction, it can be transformed into the rocksalt structure. However, this mechanism involves bond breaking and is inconsistent with the deformation of the MD cell we obtained in the MD simulation. If each sublattice shifted to the {111} direction, the MD cell would keep cubic form with the transformation.

Figure 6 shows the mechanism found in our MD simulations. When the structural transformation starts, the zinc-blende structure is compressed in one direction, and one angle between the MD cell vectors is decreased from 90° to about 70°. Accompanied by this deformation, the Si and C sublattices shift relatively to each other along the compressed direction shown by black arrows in Fig. 6. This direction is the {100} direction in the original zinc-blende structure, and the {110} direction in the transformed rocksalt structure. Figure 6 shows that the atom enclosed by a blue circle moves to a position with sixfold coordination after the transition. We should note that this transformation does not involve any bond breaking.

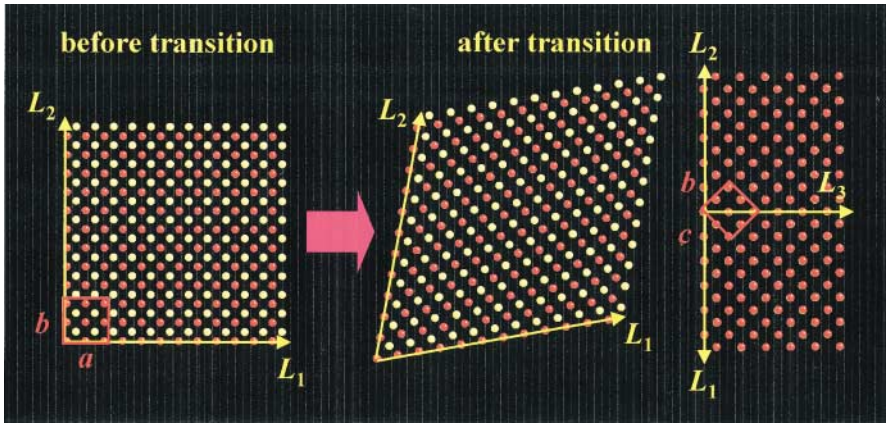

FIG. 5 (color). Average positions of atoms in the MD cell before and after the transition. The red and yellow balls show the positions of Si and C atoms, respectively. The red box shows the unit cell of each structure.

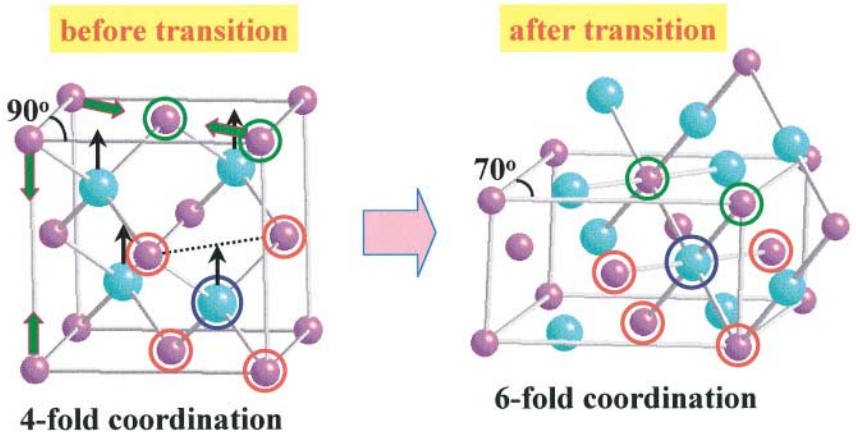

FIG. 6 (color). Microscopic mechanism of the structural transformation from the zinc-blende structure to the rocksalt structure. The blue and purple balls show the positions of Si and C atoms, respectively. The arrows show directions along which the atoms move accompanied with the transformation.

It is important to confirm that the reverse transformation from the rocksalt structure to the zinc-blende structure occurs with the present interatomic potentials. As mentioned before, silicon carbide has many polytypes, and various structures have local free-energy minimum between the rocksalt and zinc-blende structures. Since the system transforms easily into one of the local minimum structures when the pressure is decreased, MD simulations must be performed carefully to reproduce the reverse transformation. When we carried out the simulations starting from the rocksalt structure at a decreasing rate of pressure 5 GPa/48 ps, a fourfold coordinated structure was successfully reproduced at 20 GPa, although there exist some stacking faults. In the reverse transformation there is a large hysteresis, and this is in good agreement with the experimental observations [6].

In summary, we have performed isothermal-isobaric molecular-dynamics simulations for the pressure-induced structural transformation in SiC using a new interatomic potential model. The reversible transformation between the fourfold coordinated zinc-blende structure and the sixfold coordinated rocksalt structure has been successfully reproduced. When the system is transformed from the zinc-blende phase to the rocksalt phase, the MD cell is changed from cubic to monoclinic. Accompanied by this cubic-to-monoclinic deformation, Si and C sublattices shift relatively to each other along the {100} direction in the zinc-blende structure, which turns out the {110} direction in the transformed rocksalt structure. The calculated volume change at the transition and hysteresis are in good agreement with those observed in experiments.

This work was supported by NSF, DOE, AFOSR, ARO, USC-LSU Multidisciplinary University Research Initiative, and NASA. Simulations were performed using the 64-CPU Digital Alpha cluster in the Concurrent Computing Laboratory for Materials Simulations at Louisiana State University and the parallel computers at DoD's Major Shared Resource Centers under a challenge grant.

[1] R. C. Marshall, J. Faust, Jr., and C. E. Ryan, in *Silicon Carbide–1973,* edited by R. C. Marshall and J. Faust, Jr. (University of South Carolina Press, Columbia, SC, 1974), p. 671.
[2] G. R. Fisher and P. Barnes, Philos. Mag. B **61,** 217 (1990).
[3] M. W. Chase *et al.,* J. Phys. Chem. Ref. Data Suppl. **14,** 633 (1985).
[4] R. M. Wentzcovitch, C. R. S. Da Silva, N. Binggeli, and J. R. Chelikowsky, Phys. Rev. Lett. **80,** 2149 (1988).
[5] K. Strössner and M. Cardona, Solid State Commun. **63,** 113 (1987).
[6] M. Yoshida, A. Onodera, M. Ueno, K. Takemura, and O. Shimomura, Phys. Rev. B **48,** 10 587 (1993).
[7] T. Sekine and T. Kobayashi, Phys. Rev. B **55,** 8034 (1997).
[8] N. E. Christensen, S. Satopathy, and Z. Pawlowska, Phys. Rev. B **35,** 1032 (1987).
[9] K. J. Chang and M. L. Cohen, Phys. Rev. B **35,** 8196 (1987).
[10] K. Karch, F. Bechstedt, P. Pavone, and D. Strauch, Phys. Rev. B **53,** 13 400 (1996).
[11] J. Tersoff, Phys. Rev. B **39,** 5566 (1989).
[12] M. Parrinello and A. Rahman, Phys. Rev. Lett. **45,** 1196 (1980); M. Parrinello *et al.,* Phys. Rev. Lett. **50,** 1073 (1983).
[13] J. R. Ray and A. Rahman, J. Chem. Phys. **80,** 442 (1984).
[14] R. M. Wentzcovitch, Phys. Rev. B **44,** 2358 (1991).
[15] J. S. Tse, D. D. Klug, and Y. Le Page, Phys. Rev. Lett. **69,** 3647 (1992); Phys. Rev. B **46,** 5933 (1992).
[16] G. J. Martyna, D. J. Tobias, and M. L. Klein, J. Chem. Phys. **101,** 4177 (1994).
[17] M. Tuckerman, B. J. Berne, and G. J. Martyna, J. Chem. Phys. **97,** 1990 (1992).
[18] F. H. Stillinger and T. A. Weber, Phys. Rev. B **31,** 5262 (1985).
[19] P. Vashishta *et al.,* in *Amorphous Insulators and Semiconductors,* edited by M. F. Thorpe and M. I. Mitkova, NATO ASI, Ser. 3, Vol. 23 (Kluwer, Boston, 1996).
[20] W. R. L. Lambrecht, B. Segall, M. Methfessel, and M. van Schilfgaarde, Phys. Rev. B **44,** 3685 (1991).
[21] A. Taylor and R. M. Jones, in *Silicon Carbide, A High Temperature Semiconductor,* edited by J. R. O'Connor and J. Smiltens (Pergamon, New York, 1960), p. 147.